Environment Perception Using Grid Occupancy Estimation with Belief Functions

Jean Dezert, Julien Moras, Benjamin Pannetier
The French Aerospace Lab
ONERA/DTIM/EVF
F-91761 Palaiseau, France.
Email: {firstname.lastname}@onera.fr

***Abstract*—Grid map offers a useful representation of the perceived world for mobile robotics navigation. It will play a major role for the safety (obstacle avoidance) of next generations of terrestrial vehicles, as well as for future autonomous navigation systems. In a grid map, the occupancy state of each cell represents a small piece of information of the surrounding area of the vehicle. The state of each cell must be estimated from sensors measurements and classified in order to get a complete and precise perception of the dynamic environment where the vehicle moves. So far, the estimation and the grid map updating have been done using fusion techniques based on the probabilistic framework, or on the classical belief function framework thanks to an inverse model of the sensors and Dempster-Shafer rule of combination. Recently we have shown that PCR6 rule (Proportional Conflict Redistribution rule #6) proposed in DSmT (Dezert-Smarandache Theory) did improve substantially the quality of grid map with respect to other techniques, especially when the quality of available information is low, and when the sources of information appear as conflicting. In this paper, we go further and we analyze the performance of the improved version of PCR6 with Zhang's degree of intersection. We will show through different realistic scenarios (based on a LIDAR sensor) the benefit of using this new rule of combination in a practical application.**

Keywords: Information fusion, grid map, cell occupancy, perception, belief functions, DSmT, PCR6, ZPCR6.

I. Introduction

Occupancy Grids (OG) are often used for intelligent vehicle environment perception and navigation, which requires techniques for data fusion, localization and obstacle avoidance. As OGs manage a representation of the environment that does not make any assumption on the geometrical shape of the detected elements, they provide a general framework to deal with complex perception conditions. In our previous works, we did focus on the use of a multi-echo and multi-layer LIDAR system in order to characterize the dynamic surrounding environment of a vehicle driving in common traffic conditions. The perception strategy involved map estimation and scan grids [1], [2] based either on the classical bayesian framework, or on classical evidential framework based on Dempster-Shafer theory (DST) [3] of belief functions. The map grid acts as a filter that accumulate information and allows to detect moving objects. A comparative analysis of performances of these approaches has already been published recently in [4].

In dynamic environments, it is crucial to have a good modeling of the information flow in the data fusion process in order to avoid adding wrong implicit prior knowledge that will need time to be forgotten. In this context, evidential OG are particularly interesting to make a good management of the information since it is possible to explicitly make the distinction between non explored and the cells that support moving objects.

The idea of using the probabilistic framework to estimate the grid occupancy has been popularized by Elfes in his pioneered works in 1990's [8]. Later, the idea has been extended with the fuzzy logic theory framework by Oriolo et al. [10], and in parallel with the belief function (evidential) framework as well [11]–[15]. Most of the aforementioned research works dealt only with acoustic sensors (i.e SONAR). Recently, DSmT has also been applied for the perception of the environment with acoustic sensors as reported in [16]–[18].

The aim of this paper is to analyze the performance of the improved version of PCR6 taking into account Zhang's degree of intersection of focal elements (called ZPCR6 rule), which has been presented in details in the companion paper [7] in a realistic perception problem using a LIDAR sensor. We show how the environment perception with non acoustic sensors can be done, and compare the performances of different fusion rules (Bayesian, Dempster-Shafer, PCR6 and ZPCR6) in terms of accuracy of grid map estimation.

This paper is organized as follows. After a short presentation of the basics of belief functions and rules of their combination based on DST and DSmT in the next section, we will present the inverse sensor models fusion based architecture in section III. In section IV, we present an illustrating scenario for environment perception including a mobile object with a platform equipped with a LIDAR, and we compare our new realistic simulation results with those obtained by the probabilistic and the classical belief-based approaches. We will show how static and mobile objects are extracted from the occupancy grid map using digital image processing. Finally, conclusion and outline perspectives are given in section V.

II. Basics of belief functions and their fusion

Dempster-Shafer theory (DST) of evidence has been developed by Shafer in 1976 from Dempster's works [3]. DST is known also as the theory of belief functions and it is mainly characterized by a frame of discernment (FoD), sources of evidence represented by basic belief assignment (BBA), belief (Bel) and plausibility (Pl) functions, and Dempster's

rule denoted DS[1] rule of combination in the sequel. DST has been modified and extended into Dezert-Smarandache theory [6] (DSmT) to work with quantitative or qualitative BBA and to combine the sources of evidence in a more efficient way thanks to new proportional conflict redistribution (PCR) fusion rules – see [19]–[22] for discussion and examples.

A. Belief functions

Let us consider a finite discrete FoD $\Omega = \{\omega_1, \omega_2, \ldots, \omega_n\}$, with $n > 1$, of the fusion problem under consideration and its fusion space G^Ω, which can be chosen either as the power-set 2^Ω, the hyper-power set[2] D^Ω, or the super-power set S^Ω depending on the model that fits with the problem [6]. A BBA associated with a given source of evidence is defined as the mapping $m(.) : G^\Omega \rightarrow [0,1]$ satisfying $m(\emptyset) = 0$ and $\sum_{A \in G^\Omega} m(A) = 1$. The quantity $m(A)$ is called mass of belief of A committed by the source of evidence. Belief and plausibility functions are defined by

$$\text{Bel}(A) = \sum_{\substack{B \subseteq A \\ B \in G^\Omega}} m(B) \quad \text{and} \quad \text{Pl}(A) = \sum_{\substack{B \cap A \neq \emptyset \\ B \in G^\Omega}} m(B). \quad (1)$$

The degree of belief $\text{Bel}(A)$ given to a subset A quantifies the amount of justified specific support to be given to A, and the degree of plausibility $\text{Pl}(A)$ quantifies the maximum amount of potential specific support that could be given to A. If for some $A \in G^\Omega$, $m(A) > 0$ then A is called a focal element of the BBA $m(.)$. When all focal elements are singletons and $G^\Omega = 2^\Omega$ then the BBA $m(.)$ is called a Bayesian BBA [3] and its corresponding belief function $Bel(.)$ is homogeneous to a (possibly subjective) probability measure, and one has $Bel(A) = P(A) = Pl(A)$, otherwise in general one has $Bel(A) \leq P(A) \leq Pl(A)$, $\forall A \in G^\Omega$. The vacuous BBA representing a totally ignorant source is defined as $m_v(\Omega) = 1$.

B. Fusion rules

Many rules have been proposed in the literature in the past decades (see [6], Vol. 2 for a detailed list of fusion rules) to combine efficiently several distinct sources of evidence represented by the BBA's $m_1(.)$, $m_2(.)$, ..., $m_s(.)$ ($s \geq 2$) defined on same fusion space G^Ω. In this paper, we focus only on DS rule because it has been historically proposed in DST and it is still widely used in applications, and on the PCR rule no. 6 (i.e., PCR6) proposed in DSmT because it provides a very interesting alternative of DS rule, even if PCR6 is more complex to implement in general than DS rule.

In DST framework, the fusion space G^Ω equals the power-set 2^Ω because Shafer's model of the frame Ω is assumed, which means that all elements of the FoD are exhaustive and exclusive. The DS combination of the BBA's $m_1(.)$ and $m_2(.)$, is defined by taking $m_{1,2}^{DS}(\emptyset) = 0$, and for all $X \neq \emptyset$ by in 2^Ω

$$m_{1,2}^{DS}(X) \triangleq \frac{1}{1 - m_{1,2}(\emptyset)} \sum_{\substack{X_1, X_2 \in 2^\Omega \\ X_1 \cap X_2 = X}} \prod_{i=1}^{2} m_i(X_i), \quad (2)$$

where the numerator of (2) is the mass of belief on the conjunctive consensus on X. The denominator $1 - m_{1,2}(\emptyset)$ is a normalization constant. The total degree of conflict between the two sources of evidences is classically defined by

$$m_{1,2}(\emptyset) \triangleq \sum_{\substack{X_1, X_2 \in 2^\Omega \\ X_1 \cap X_2 = \emptyset}} \prod_{i=1}^{2} m_i(X_i). \quad (3)$$

According to Shafer [3], the two sources are said to be in total conflict if $m_{1,2}(\emptyset) = 1$. In this case the combination of the sources by DS rule cannot be done because of the mathematical 0/0 indeterminacy. $m_{1,2}^{DS}(.)$, when it is mathematically defined, is a true normalized belief mass function as defined in Section II-A. The vacuous BBA $m_v(\Omega) = 1$ is a neutral element for DS rule. This rule is commutative and associative, and the formula (2) can be easily generalized for the combination of any number s ($s > 2$) of sources of evidences. DS rule remains the milestone fusion rule of DST.

The doubts of the validity of DS rule has been discussed by Zadeh [28]–[30] based on a very simple example with two highly conflicting sources of evidences. Since the 1980's, different authors criticized the behavior and the justification of such a DS rule. More recently, Dezert et al. in [19], [20] have shown disputable behaviors of DS rule even in low conflicting cases due to serious flaws in logical foundations of DST [21]. To overcome the limitations and problems of DS rule of combination, a new family of PCR rules have been developed in the DSmT framework. We present the most elaborate one, i.e. the PCR6 fusion rule, which has been used in our perception application for grid occupancy estimation.

In PCR rules, instead of following the DS normalization (the division by $1 - m_{1,2}(\emptyset)$), we transfer the conflicting mass only to the elements involved in the conflict and proportionally to their individual masses, so that the specificity of the information is entirely preserved. The general principle of PCR consists: 1) to apply the conjunctive rule, 2) to calculate the total or partial conflicting masses, 3) then redistribute the (total or partial) conflicting mass proportionally on non-empty sets according to the integrity constraints one has for the frame Ω. Because the proportional transfer can be done in different ways, there exist several versions of PCR rules of combination. For example, Smarandache and Dezert [6] Vol. 2, Chap. 1 proposed PCR5 rule, and Martin and Osswald in [6] Vol. 2, Chap. 2 proposed PCR6 rule. because PCR6 was more stable than PCR5 in term of decision for combining $s > 2$ sources of evidence. When only two sources are combined, PCR6 and PCR5 fusion rules coincide, but they differ as soon as more than two sources have to be combined altogether. Recently, it has been proved in [22] that only the PCR6 rule

[1]DS acronym standing for *Dempster-Shafer* since Dempster's rule has been widely promoted by Shafer in the development of his mathematical theory of evidence [3].

[2]which corresponds to a Dedekind's lattice, see [6] Vol. 1.

is consistent with the averaging fusion rule which allows to estimate the empirical (frequentist) probabilities involved in a discrete random experiment. For Shafer's model of FoD[3], PCR6 fusion of two BBA's $m_1(.)$ and $m_2(.)$ is defined by $m_{1,2}^{PCR6}(\emptyset)=0$ and for all $X\neq\emptyset$ in 2^Ω

$$m_{1,2}^{PCR6}(X)=\sum_{\substack{X_1,X_2\in 2^\Omega\\ X_1\cap X_2=X}} m_1(X_1)m_2(X_2) + \sum_{\substack{Y\in 2^\Omega\setminus\{X\}\\ X\cap Y=\emptyset}} [\frac{m_1(X)^2m_2(Y)}{m_1(X)+m_2(Y)}+\frac{m_2(X)^2m_1(Y)}{m_2(X)+m_1(Y)}], \quad (4)$$

where all denominators in (4) are different from zero. If a denominator is zero, that fraction is discarded[4]. All propositions/sets are in a canonical form [6]. Very basic Matlab codes of PCR rules can be found in [6], [23] and from the toolboxes repository on the web [27]. Like the averaging fusion rule, the PCR6 fusion rule is commutative but not associative. The vacuous belief assignment is a neutral element for this rule.

The PCR6 rule of combination (as well as DS rule) use only part of the whole information available (i.e., the values of the masses of belief only), and they do not exploit the cardinalities of focal elements entering in the fusion process. Because the cardinalities of focal elements are fully taken into account in the computation of the measure of degree of intersection between sets, we have recently proposed to improve PCR6 rules using this measure in the companion paper [7]. The basic idea is to replace any conjunctive product by its discounted version thanks to the measure of degree of intersection D when the intersection of focal elements is not empty. The product of partial (or total) conflicting masses are not discounted by the measure of degree of intersection because the degree of intersection between two (or more) conflicting focal elements always equals zero, that is if $X\cap Y=\emptyset$, then $D(X,Y)=0$. In [7], we have shown in different examples why Zhang's *degree of intersection* [31], denoted $D^Z(X_1,\ldots,X_s)$, is more interesting than classical Jaccard's degree [32]. $D^Z(X_1,\ldots,X_s)$ is mathematically defined by

$$D^Z(X_1,\ldots,X_s)\triangleq\frac{|X_1\cap X_2\cap\ldots\cap X_s|}{|X_1|\cdot|X_2|\cdot\ldots\cdot|X_s|}, \quad (5)$$

where $|X_1\cap X_2\cap\ldots\cap X_s|$ is the cardinality of the intersection of the focal elements X_1, X_2,..., X_s, and $|X_1|$, $|X_2|$, $\ldots|X_s|$ their cardinalities. The improved version of PCR6 with Zhang's degree of intersection (called ZPCR6 rule) is easy to compute and it corresponds to the following formula[5]

$$m_{1,2}^{ZPCR6}(X)=\frac{1}{K_{1,2}^{ZPCR6}}\cdot \Big[\sum_{\substack{X_1,X_2\in 2^\Omega\\ X_1\cap X_2=X}} D^Z(X_1,X_2)m_1(X_1)m_2(X_2) + \sum_{\substack{Y\in 2^\Omega\setminus\{X\}\\ X\cap Y=\emptyset}} [\frac{m_1(X)^2m_2(Y)}{m_1(X)+m_2(Y)}+\frac{m_2(X)^2m_1(Y)}{m_2(X)+m_1(Y)}]\Big], \quad (6)$$

where $K_{1,2}^{ZPCR6}$ is a normalization constant such that $\sum_{X\in 2^\Omega} m_{1,2}^{ZPCR6}(X)=1$. As for PCR6, one has $m_{1,2}^{ZPCR6}(\emptyset)=0$ and ZPCR6 is commutative but not associative. The advantage of ZPCR6 over PCR6 and DS rules is its ability to respond to the inputs in a more effective way has clearly shown in examples in [7].

C. Discounting

A discounting effect can be applied on a mass function $m(.)$ if a piece of information has its reliability lowered. In this case, a new mass function $m_\alpha(.)$ (with $\alpha\in[0,1]$) is computed from $m(.)$ and a part of the mass of each element of the FoD is transferred to the whole FoD Ω which represents the total ignorance. More precisely, one defines

$$m_\alpha(A)\triangleq\begin{cases}(1-\alpha)\cdot m(A) & if\ A\neq\Omega\\ (1-\alpha)\cdot m(A)+\alpha & if\ A=\Omega\end{cases}. \quad (7)$$

III. Evidential Occupancy Grid

The basic idea of an Occupancy Grid (OG) is to divide the surrounding environment (the ground plane of the 2D world) into a set a cells (denoted C^i, $i\in[0,n]$ for convenience) in order to estimate their occupancy state. Each cell C_{ij} of the perception grid represents a square over the ground place defined by the cordinates : $[x_0-i\cdot\delta/2, x_0+i\cdot\delta/2]\times[y_0-j\cdot\delta/2, y_0+j\cdot\delta/2]$, where (x_0,y_0) represents the origin of the frame of the occupancy grid and δ the grid resolution. In a probabilistic framework, the aim is to estimate the probabilities $P\left(O^i|z_{1:t}\right)$ and $P\left(F^i|z_{1:t}\right)$ given a set of measures $z_{1:t}$ from the beginning up to the current time t. O^i (resp. F^i) denotes the occupied (resp. free) state of the cell C^i. Finally, a decision rule is applied to select the most likely state for each cell.

For the evidential approach, and occupancy grid represents the information using a mass function over the frame of discernment (FoD) $\Omega=\{F,O\}$ and the occupancy of each cell C_{ij} is represented by its associeted mass $m_{ij}(.)$. So the mass functions used in grid have the structure

$$m_t=\left[\begin{array}{cccc} m_t(\emptyset) & m_t(F) & m_t(O) & m_t(\Omega)\end{array}\right]. \quad (8)$$

The occupancy mass function can be used during the fusion process, then the decision can be taken using pignistic transform [26] to get a probability measure and use the same decision rule but an evidential decision rule can also be applied directly on the mass function. An interesting part of

[3]that is when $G^\Omega=2^\Omega$, and assuming all elements exhaustive and exclusive.

[4]If a denominator, e.g., $m_1(X)+m_2(Y)$ tends towards 0, then also the conflicting mass $m_1(X)m_2(Y)$ that is transferable tends to zero because $m_1(X)$ and $m_2(Y)$ tend to zero (since they are positive), therefore the redistribution masses also tend to zero. That reflects the continuity of PCR6.

[5]The general ZPCR6 formula for $s>2$ sources in detailed in [7].

an evidential occupancy grid is that the FoD can be more complex, and as the fusion is done cell by cell the fusion scheme will be still valid.

Occupancy grids updating strategies can be classified into two categories depending on the use of a forward or inverse sensor model. The forward model relies on Bayes inference. Since this approach takes into account the conditional dependency of the cells of the map, it is well adapted to a sensor that observes a large domain of cells with only one reading measurement (e.g., an ultrasonic sonar). However, it requires heavy processing that can be handled by optimized approximation. The inverse model approach is well adapted to narrow fields of measure by sensors (e.g., LIDAR). It is composed of two separate steps. First, a snapshot map of the sensor reading is built using an inverse sensor model $P\left(O^i|z_t\right)$, which takes into account the conditional dependency between the sensor reading and the occupancy of the seen cells. Then, a fusion process (denoted $\odot$) is done with the previous map $P\left(O^i|z_{1:t-1}\right)$ as an independent opinion poll fusion:

$$P\left(O^i|z_{1:t}\right) = P\left(O^i|z_t\right) \odot P\left(O^i|z_{1:t-1}\right). \tag{9}$$

In the probabilistic framework, the usual fusion operation between states A and B coming from an independent measurement, uses the independent opinion poll [35]:

$$P(A) \odot P(B) = \frac{P(A)P(B)}{P(A)P(B) + (1 - P(A))(1 - P(B))}. \tag{10}$$

Inverse approaches have very efficient implementations (e.g., log-odd) that make them popular in mobile robotics [8], [9], [25]. Maps built using inverse models are usually less accurate, since they just take into account the dependency of the cells observed in one reading. They provide a good approximation with accurate and high resolution sensors observing a limited number of cells at a time.

A. Fusion strategy with the inverse model

When dealing with the inverse model approach, an estimate of the pose of the robot has to be available, and a map grid G^M has to be handled. This grid is defined in a world-referenced frame (so it does not move with the robot) and it is updated when a new sensor reading is available. Because of the likely evolution of the world in a dynamic environment, the OG update has to be completed by a remanence strategy. The fusion architecture is based on a prediction-correction paradigm to fuse one or several sensors observations.

a) Prediction step: The prediction step computes the predicted map grid at time t from the map grid estimated at time $t-1$. Depending on the available information, this step can be very refined as done in [24]. Because we do not have specific information on the velocity of the objects (or cells), the prediction step is done by the classical discounting technique. The confidence in past data is controlled by a remanence factor $\alpha \in [0; 1]$. The prediction stage is therefore governed by

$$\hat{G}^M_{t|t-1} = discount\left(\hat{G}^M_{t-1|t-1}, \alpha\right). \tag{11}$$

b) Correction step: The correction step consists in the combination of the previously estimated map grid with the grid built from the current measures thanks to the inverse model sensor (see more details in [1], [2]). This one is called ScanGrid G^S_t. As this information is referenced in the sensor frame, a 2D warping is applied to reshape this grid into the fusion frame. To do this, the pose of the robot provided by an accurate localisation system (i.e GPS aided by odometry or LIDAR SLAM algorithm) is used in order to compute the motion matrix H_t as follow:

$$H_t = \begin{bmatrix} \cos(\theta_t) & -\sin(\theta_t) & T^x_t \\ \sin(\theta_t) & \cos(\theta_t) & T^y_t \\ 0 & 0 & 1 \end{bmatrix}, \tag{12}$$

where θ_t represents the heading angle of the vehicle relative to the grid frame, and the vector (T^x, T^y) represents the position of the vehicle.

An extrinsic calibration matrix C (which is also a homogeneous transformation matrix) is defined in order to compensate the position of the sensor mounted on the vehicle. A calibration step is required to compute the parameters, but in our experiment, we simply set it by hand (mesuring the position of the sensor relatively to the main frame). Finally, a matrix P is defined to warps the cordinates from world frame to grid indices. The motion matrix H_t and the extrinsic calibration matrix C are used to compute a remapping function $f(i, j)$ according to Eq. (13) below:

$$f(i, j) = P \cdot C \cdot H_t \cdot P^{-1} \cdot \begin{bmatrix} i \\ j \\ 1 \end{bmatrix}. \tag{13}$$

Finally, the ScanGrid is remapped with f and fused with the previous map grid according to the general formula

$$\hat{G}^M_{t|t}(i, j) = \hat{G}^M_{t|t-1}(i, j) \odot G^S_t\left(f(i, j)\right), \tag{14}$$

where the grid G^S_t represents the BBA produced by the sensor model. This BBA is created in respect to sensor data (e.g., LIDAR point here) and a sensor model to infer an instant occupancy grid. With the probabilistic approach, it refers to the occupancy probability $P^S_t(O)$. With the evidential approach it refers to the occupancy mass function $m^S_t = \left[\begin{array}{cccc} m^S_t(\emptyset) & m^S_t(F) & m^S_t(O) & m^S_t(\Omega) \end{array}\right]$. The grid $\hat{G}^M_{t|t-1}$ refers to the previous MapGrid $\hat{G}^M_{t-1|t-1}$ predicted at current time t using Eq. (11). In the next parts, for each approach considered, the fusion rule $\odot$ used in Eq. (14) is different. Bayesian approach uses Eq.(10), DS rule Eq.(2), PCR6 rule Eq.(4), and ZPCR6 rule Eq.(6).

B. Discounting in Occupancy Grids

The main advantage of using discounting is to provide a simple way to model the presence of dynamic object in the scene. The discounting allows to make a prediction without needing information on the dynamic at the cell level (or at the object level). The information on the dynamic of objects in the environment is rarely available from sensors, and the dynamic is difficult to estimate without greedy time-computing

algorithms [24]. The main issue with the discounting effect is that it makes impossible to build persistent static map. Indeed, cells not viewed by the sensor will quickly converge to the ignorance state, so this strategy cannot be used to build the map of a building for instance. If we are interested to build static map in presence of moving objects, the discounting function is then not recommended. We will see why in the next part of the paper where in this case Bayesian and DS fusion rules will not be very efficient. To handle this case, it is recommended to use either PCR6 or ZPCR6 rules.

IV. Simulation results

In this section, we present simulation results of grid occupancy estimation in a realistic scenario based on different rules of combination (Bayesian fusion, DS rule, PCR6 and ZPCR6 fusion rules).

A. Basic simulation

Setup: In order to present the basic behavior of the different combination rules studied, we have implemented at first some simple 1D-simulations, where we consider a grid cell crossed by a moving object. In this case, the state of the cell changes from free-state to occupied-state at time t_1 and from occupied-state to free-state at time t_2. The figures 1–4 show the results of these simulations under different conditions.

On each subfigure, we show on the top row the real state of the cell (i.e., the ground truth). The second row shows the sensor data simulated that correspond to the BBA of the state of the cell. This mass function is built according to the state of the cell, the level of confidence of the sensor and can be eventually perturbed with additional noises. FA indicates the rate of False Alarms and ND the rate of Non Detections. We will consider different level of confidence for $m_{SG}(O)$ when the cell is occupied and $m_{SG}(F)$ when the cell if free. The subfigures at the bottom represent the level of belief of the cell state obtained with Bayesian fusion, DS rule, PCR6 and ZPCR6 fusion rules.

Effect of discounting: Fig.1 shows the results of the classical chain using a discounting factor $\alpha = 0.05$ while Fig. 2 is the same case without discounting ($\alpha = 0$). Without discounting, a lag appears with Bayesian and DS fusion rules. The lag is seriously reduced with PCR6 and ZPCR6. We insist on the fact that PCR6 and ZPCR6 rules allow to estimate efficiently the moving objects in the grid without using discounting. With discounting, all the fusion rules behave similarly, but because of memory vanishing effect due to the discounting we forget what has been perceived before which prevents us to map efficiently the whole perceived environment. Fortunately, this unsatisfying behavior (for a mapping purpose standpoint) can be avoided if ones uses PCR6 or ZPCR6 without discounting.

Performances analyses: To evaluate the performance of our method, we did perform 10000 Monte Carlo runs for each simulation in order to estimate the false alarm and non detection rates. In order to make the decision, the pignistic probability has been computed and a MAP estimator has been used. Each simulation (from No 0 to No 8) corresponding to different conditions (the discounting level, the rate of noise impacting the sensor observations) is reported in Table I. For each simulation presented in the Table I, we obtain the performances (rates of FA and ND in %) shown in Table II.

Simulations 0 and 1 illustrated by Figures 1 and 2, correspond to the noise-free situation. By removing the discounting operator, Bayesian and DS approaches have a lag in the detection of the change of state that impacts clearly their performances. The PCR6 and ZPCR6 approach are not concerned by this effect because of PCR of conflict. Simulations 2 and 3 (see Fig. 3) include 10% of wrong measurement caused by noises. The fusion rules behave similarly as for simulations 0 and 1, but the performances are a bit lower which shows the effect of noisy measurements in the estimation process.

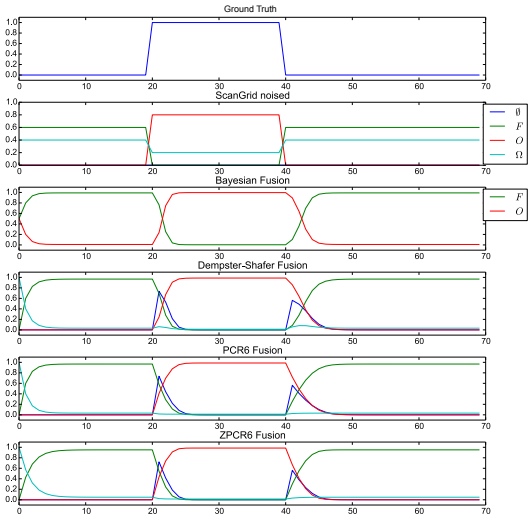

Fig. 1. Case with discounting ($\alpha = 0.05$).

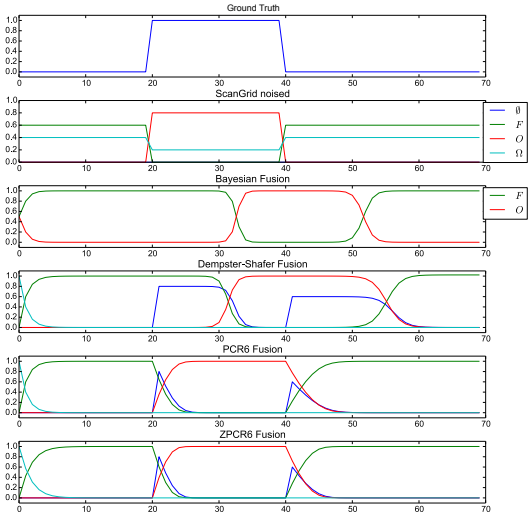

Fig. 2. Case without discounting ($\alpha = 0$).

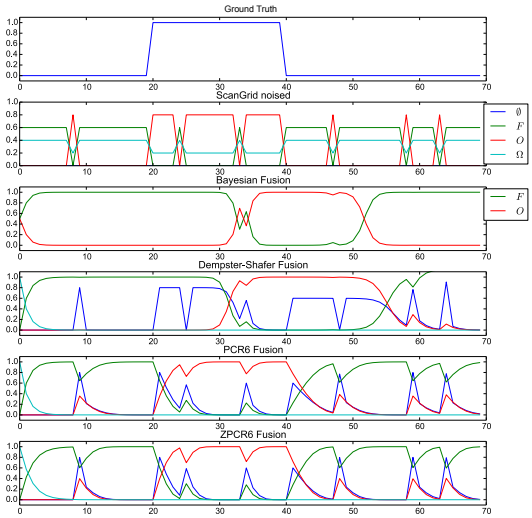

Fig. 3. Case with noise (FA=10%, ND=10%) and $\alpha = 0$.

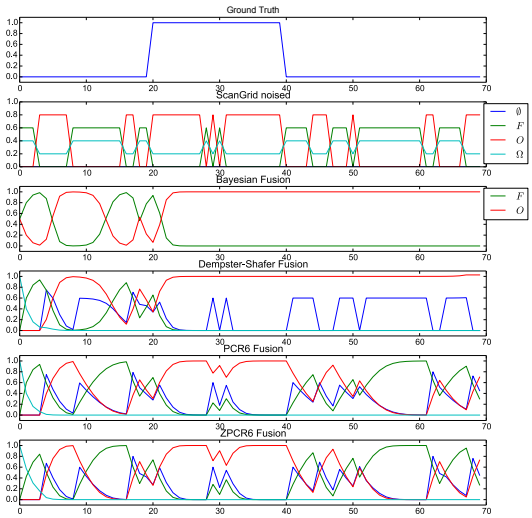

Fig. 4. Case with noise (FA=30%, ND=15%) and $\alpha = 0$.

Simu N°	discounting	sensor noise	sensor belief
	α	ND/FA	$m_{SG}(O)/m_{SG}(F)$
0	0.05	0	0.8/0.6
1	0	0	0.8/0.6
2	0.05	10/10	0.8/0.6
3	0	10/10	0.8/0.6
4	0.05	15/30	0.8/0.69
5	0	15/30	0.8/0.68
6	0	15/30	0.6/0.4
7	0	25/50	0.6/0.4
8	0	25/50	0.4/0.2

TABLE I
PARAMETERS OF SIMULATIONS.

For simulations 4, 5 and 6, the noise reaches 15% for ND and 30% for FA which is important. As we see in Fig. 4, the Bayesian and DS fusion rules are not able to detect the second state change, during the simulation time. This induces the bad false alarm rates. In the last simulations 7 and 8 the noise is very important (about 25% of ND and 50% of FA). In these conditions, all the methods have poor false alarm rates but the PCR6 and ZPCR6 keep good non detection rates. Globally, we see an improvement of the performances when using ZPCR6, especially for the reduction of the FA rates.

Simu #	Bayesian		DS		PCR6		ZPCR6	
	ND	FA	ND	FA	ND	FA	ND	FA
0	10.0	6.0	10.0	6.0	10.0	6.0	10.0	4.0
1	65.0	24.0	60.0	32.0	10.0	6.0	10.0	4.0
2	11.2	9.2	10.5	10.0	10.0	9.6	11.1	7.8
3	77.7	15.2	73.5	18.9	11.5	6.7	11.3	7.5
4	9.2	28.0	8.2	31.5	8.4	28.9	9.8	25.8
5	33.0	62.7	26.9	65.8	8.4	28.8	10.1	24.7
6	31.3	63.9	26.0	67.3	9.3	38.7	8.8	32.3
7	15.1	76.9	11.5	79.4	5.7	64.0	7.5	55.2
8	7.1	83.9	5.1	85.1	1.9	87.3	3.0	76.2

TABLE II
RATES OF FALSE ALARM AND NON DETECTION (IN %).

B. LIDAR simulation

Here, the DS and PCR6 fusion rules are compared on a 2D occupancy grid problem close to real application for robot perception. The simulation has been done using the Robot Operating System (ROS) [33] environment and the Gazebo [34] simulator is used here to simulate a Hokuyo LIDAR and a moving object as shown on Figure 5. The simulated sensor has a FoV (Field of View) about 270° and a max range of about 10m. The rate of the scan is 20Hz and the ranges of the LIDAR point is corrupted with a Gaussian noise $\mathcal{N}(0, 0.1)$.

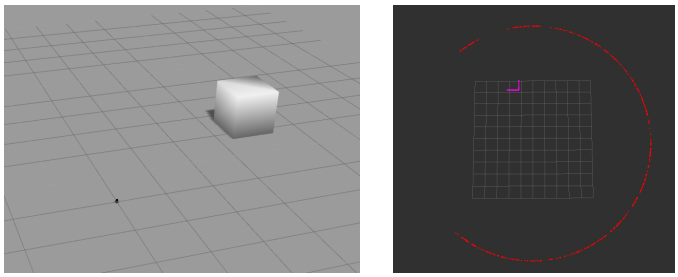

Fig. 5. Gazebo simulation: the box turns around the LIDAR sensor. Left: 3D view of the simulation scene, Right: view of one Lidar scan (bird view).

Figure 5 shows a simulated scan. The beams that do not hit obstacle within the range are considered as max range (as done in the real Hokuyo sensor). The moving object is a box moving circularly at 6rpm around the LIDAR. A *ground truth* grid is computed according the real position of the box and its geometry at each scan time. The grid used is a square of 10m by 10m with a resolution of 0.1m and the ScanGrid BBA are set to $m_{SG}(O) = 0.8$, $m_{SG}(\Omega) = 0.2$ for occupied cells, and $m_{SG}(F) = 0.6$, $m_{SG}(\Omega) = 0.4$ for free cells.

In order to quantify the results, we compute some metrics. However, because of occlusion, only the cells located on the edges of the box can be considered, that is why we do not use global metrics. We use the following metrics: 1) the number of correct occupied cell (proportional to recall in our case), and 2) the number of conflicting cells close to the box. The

first describes the ability of the method to add objects into the map, and also by analogy to remove an object from the map. The second describes the ability of the method to detect moving objects by generating conflict. This ability is important and shows the improvements of the evidential grid over the classical Bayesian grid. The number of cells detected for both metrics depends a lot on the position around the sensor. This dependency exists because the LIDAR sensor is able to see two edges of the box in some cases, or only one edge in other situations, and even no edge at all if the box is out of its field of view (when the box is located behind the LIDAR sensor).

Figure 6 shows that the number of occupied cells with the ZPCR6 is very close to the one obtained with PCR6, but slightly higher. DS fusion without discounting can not handle well the quick change of states in the map.

Figure 7 shows the number of cells that support conflict which also fit into the box shape generated from the Ground Truth. DS approach generates more conflicting cells than PCR6 and ZPCR6 because it does not provide occupied cells. As we see, PCR6 and ZPCR6 allow also to generate conflicting cells corresponding to the moving object that may be sufficient to identify them as *moving cells*. In this case, PCR6 performs slightly higher than ZPCR6.

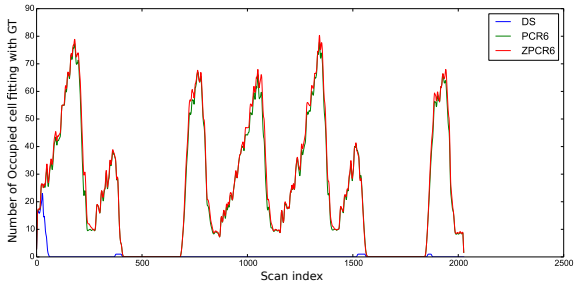

Fig. 6. 2D LIDAR Simulation: Number of correct occupied cells (blue=DS rule, green=PCR6 rule, red=ZPCR6 rule).

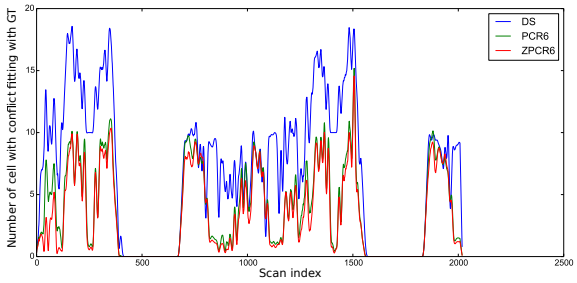

Fig. 7. 2D LIDAR Simulation: Number of cells with conflict that fit with the ground gruth (blue=DS rule, green=PCR6 rule, red=ZPCR6 rule).

C. Real data processing

A real experiment was done using an Hokuyo UTM-30LX sensor. This experiment takes place in an office in which a person was walking into. The room is rectangular but there are furnitures in it (desk, armchairs, wall cabinets, etc) with windows and the door was open. In our experiment, a person was walking around the desk in the office room. The evidential occupancy grid fusion node was implemented within the ROS environment. The grid has the same size and resolution as in the previous example. The BBA used in the sensor model has been set to $m_{SG}(O) = 0.8$, $m_{SG}(\Omega) = 0.2$ for occupied cells and $m_{SG}(F) = 0.86$, $m_{SG}(\Omega) = 0.2$ for free cells. No discounting was applied.

Figures 8–10 present the occupancy grid estimation using DS, PCR6 and ZPCR6 rules for a typical snapshot of the sequence. The color of cells denotes the state having the highest mass value: green for F (free state), red for O (occupied state), and black for Ω (full uncertainty). For convenience, we have also displayed in blue all the cells that carry a conflicting mass $m(\emptyset) > 0$ before applying the normalization step of DS rule, or before applying the proportional conflict redistribution with PCR6, or both with ZPCR6.

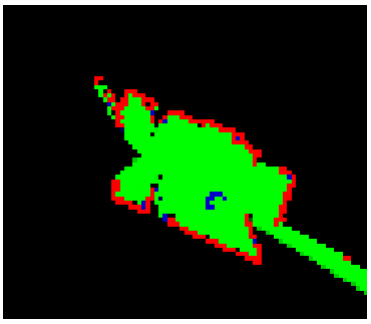

Fig. 8. Snapshot 1 - with DS fusion.

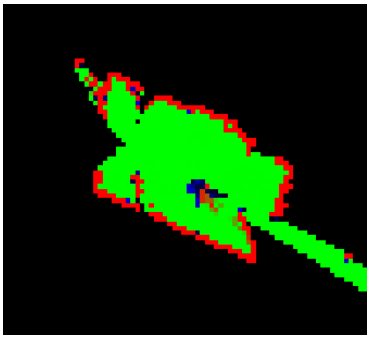

Fig. 9. Snapshot 1 - with PCR6 fusion.

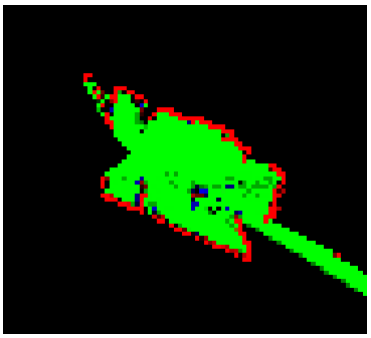

Fig. 10. Snapshot 1 - with ZPCR6 fusion.

Figure 8 shows the result using DS rule. The room scanned by the sensor is correctly mapped and its bounds (mainly walls

and doors) are clearly identified by the red pixels. The free space (green pixels) is correctly detected in the room except near the person that is labeled as free (with conflicting cell shown in blue for convenience). The person moving around the desk in the office room is only detected from conflicting cells when he stops to walk several times.

Figure 9 shows the PCR6 result at the same time stamps. In this case, the person is rightly detected as shown by the red pixels (occupied cells) inside the green area (the office room). A conflict cell is created when he starts walking in the room. The static part of the room is also detected (as with DS fusion rule). Figure 10 shows the ZPCR6 result at the same time stamps. The results of this rule are close to the PCR6 rule but the level of ignorance (the mass on Ω) is higher on the cells behind the person. This can be understood because the mass $m(\Omega)$ is weighed by a factor 0.5 during the transition.

V. Conclusions and perspectives

In this work we have presented a novel application of the belief functions which significantly improves the map building process for intelligent vehicles environment perception and grid map estimation. This work shows the importance of defining an accurate sensor model. We have considered the uncertainties of the LIDAR measurements and used the ZPCR6 rule of DSmT to model and combine sensor information. Our new method differs from Bayesian approach by allowing support for more than one proposition at a time, rather than a single hypothesis. It is a interval-based approach, as defined by the lower and upper probability bounds $[\text{Bel}, \text{Pl}]$ allowing the lack of measurement to be modeled adequately. This new method based on ZPCR6 rule differs from the classical evidential approach based on DS rule and improves in theory the results based PCR6, and more substantially the results of DS rule. Our experimental results with the LIDAR confirm the improvement of the accuracy of this new grid estimation method w.r.t previous methods, but the improvment obtained with ZPCR6 over PCR6 is not so important because of the too simplistic structure of the chosen frame of discernment. As research perspectives, we will try to implement these fusion rules in 3D occupancy grid (Octomap based) and use a stereo camera with dense disparity map computation as sensor source. Also we would like to deal with refined frames of discernment to ameliorate the precision of the perception and to emphasize the advantages of ZPCR6 rule.

References

[1] J. Moras, V. Cherfaoui, P.Bonnifait, *Credibilist occupancy grids for vehicle perception in dynamic environments*, 2011 IEEE Int. Conf on Robotics and Automation, Shanghai, China, pp. 84–89, May 2011.

[2] J. Moras, V. Cherfaoui, P. Bonnifait, *Moving Objects Detection by Conflict Analysis in Evidential Grids*, 2011 IEEE Intelligent Vehicles Symposium IV, pp. 1122–1127, June 2011.

[3] G. Shafer, *A Mathematical Theory of Evidence*, Princeton: Princeton University Press, 1976.

[4] J. Moras, V. Cherfaoui, P. Bonnifait, *Evidential Grids Information Management in Dynamic Environments*, Fusion 2014, Spain, July 2014.

[5] J. Moras, J. Dezert, B. Pannetier, *Grid occupancy estimation for environment perception based on belief functions and PCR6*, Proc. of SPIE (SP/SIF, and Target Recogn. XXIV), USA, 20–22 April 2015.

[6] F. Smarandache, J. Dezert (Editors), *Advances and applications of DSmT for information fusion (Collected works)*, American Research Press, USA Vol.1–4, 2004–2015. http://www.onera.fr/staff/jean-dezert?page=2

[7] F. Smarandache, J. Dezert, *Modified PCR Rules of Combination with Degrees of Intersections*, in Proc. of Fusion 2015, USA, July 6-9, 2015.

[8] A. Elfes, *Using occupancy grids for mobile robot perception and navigation*, Computer, Vol. 22, no. 6, pp. 46–57, 1989.

[9] H.P. Moravec, *Sensor fusion in certainty grids for mobile robots*, AI Magazine, Summer: 116–121, 1988.

[10] G. Oriolo, G. Ulivi, M. Vendittelli, *On-line map building and navigation for autonomous mobile robots*, Proc. 1995 IEEE Int. Conf. on Robotics and Automation, pp. 2900–2906, Nagoya, Japan, 1995.

[11] K. Hughes, R. Murphy, *Ultrasonic robot localization using Dempster-Shafer theory*, in Proc. of SPIE on Neural and Stochastic Methods in Image and Signal Processing, 1992, pp. 2–11, 1992.

[12] P. Tirumalai, B.G. Schunk, R.C. Jain, *Evidential reasoning for building environment maps*, IEEE Trans. on SMC, Vol. 25(1), pp. 10–20, 1995.

[13] F. Gambino, G. Oriolo, G. Ulivi, *A comparison of three uncertainty calculus techniques for ultrasonic map building*, SPIE Int. Symp. on Aerospace/Defense Sensing and Control, pp. 249–260, USA, 1996.

[14] D. Pagac, E. Nebot, H. Durrant-Whyte, *An evidential approach to probabilistic map-building*, Proc. of IEEE Int. Conf. on Robotics and Automation, Vol. 1, pp. 745–750, Minneapolis, MN, USA, April 1996.

[15] T. Reineking, J. Clemens, *Evidential FastSLAM for grid mapping*, Proc. of Fusion 2013 Conf., pp. 789–796, Istanbul, Turkey, July 2013.

[16] X. Li, X. Huang, M. Wang, J. Xu, H. Zhang, *DSmT Coupling with PCR5 for Mobile Robots Map Reconstruction*, Proc. of 2006 Int. Conf. on mechatronics and Automation, Luoyang, China, June 26–28, 2006.

[17] P. Li, X. Huang, S. Yang, J. Dezert, *SLAM and path planning of mobile robot using DSmT*, J. of Soft. Eng., Vol. 7, No. 2, pp. 46–67, 2013.

[18] J. Zhou, J. Duan, G. Yang, *Occupancy Grid Mapping Based on DSmT for Dynamic Environment Perception*, Int. J. of Robotics and Automation (IJRA), Vol. 2, No. 4, pp. 129–139, Dec. 2013.

[19] J. Dezert, P. Wang, A. Tchamova, *On the validity of Dempster-Shafer theory*, Proc. of Fusion 2012 Int. Conf., Singapore, July 9–12, 2012.

[20] A. Tchamova, J. Dezert, *On the behavior of Dempster's Rule of combination and the foundations of Dempster-Shafer theory*, 6th IEEE Int. Conf. on Int. Syst. (IS'12), Sofia, Bulgaria, Sept. 6–8, 2012.

[21] J. Dezert, A. Tchamova, *On the validity of Dempster's fusion rule and its interpretation as a generalization of Bayesian fusion rule*, Int. J. of Intelligent Systems, Vol. 29(3), pp. 223–252, March 2014.

[22] F. Smarandache, J. Dezert, *On the consistency of PCR6 with the averaging rule and its application to probability estimation*, Proc. of Fusion 2013, Istanbul, Turkey, July 2013.

[23] F. Smarandache, J. Dezert, J.-M. Tacnet, *Fusion of sources of evidence with different importances and reliabilities*, Proc. of Fusion 2010 Int. Conf., Edinburgh, UK, July 26–29, 2010.

[24] M.K. Tay, et al., *The Bayesian occupation filter*, in Proba. Reas. and Dec. Making in Sensory-Motor Syst., pp. 77–98, Springer, 2008.

[25] T. Weiss, B. Schiele, K.Dietmayer, *Robust Driving Path Detection in Urban and Highway Scenarios Using a Laser Scanner and Online Occupancy Grids*, IEEE Intel. Vehicles Symp., pp. 184–189, June 2007.

[26] P. Smets, *Decision making in the TBM: the necessity of the pignistic transformation*, IJAR, Vol. 38, pp. 133–147, Feb. 2005.

[27] http://bfasp.iutlan.univ-rennes1.fr/wiki/index.php/Toolboxes

[28] L.A. Zadeh, *On the validity of Dempster's rule of combination*, Memo M79/24, Univ. of California, Berkeley, CA, U.S.A., 1979.

[29] L.A. Zadeh, *Book review: A mathematical theory of evidence*, The Al Magazine, Vol. 5, No. 3, pp. 81-83, 1984.

[30] L.A. Zadeh, *A simple view of the Dempster-Shafer theory of evidence and its implication for the rule of combination*, The Al Magazine, Vol. 7 (2), pp. 85–90, 1986.

[31] L. Zhang, *Representation, independence and combination of evidence in Dempster-Shafer theory*, in Advances in DST, Wiley, pp. 51–95, 1994.

[32] P. Jaccard, *Etude comparative de la distribution florale dans une portion des Alpes et du Jura*, Bulletin de la Société Vaudoise des Sciences Naturelles, Vol. 37, pp. 547–579, 1901.

[33] M. Quigley et al., *ROS: an open-source Robot Operating System*, ICRA Workshop on Open Source Software, 2009.

[34] N. Koenig, A. Howard, *Design and Use Paradigms for Gazebo, An Open-Source Multi-Robot Simulator*, in 2004 IEEE/RSJ Int. Conf. on Intell. Robots and Syst., pp. 2149–2154, Sept. 2004.

[35] R.A. Jacobs, *Methods for combining expert's probability assessments*, Neural Computation, Vol. 7 (5), pp. 867–888, 1995.